



HAL
open science

Multi-omics analysis of hiPSCs-derived HLCs matured on-chip revealed patterns typical of liver regeneration

Mathieu Danoy, Yannick Tauran, Stéphane Poulain, Rachid Jellali, Johanna Bruce, Marjorie Leduc, Morgane Le Gall, Françoise Gilard, Taketomo Kido, Hiroshi Arakawa, et al.

► To cite this version:

Mathieu Danoy, Yannick Tauran, Stéphane Poulain, Rachid Jellali, Johanna Bruce, et al.. Multi-omics analysis of hiPSCs-derived HLCs matured on-chip revealed patterns typical of liver regeneration. *Biotechnology and Bioengineering*, In press, 10.1002/bit.27667 . hal-03288795

HAL Id: hal-03288795

<https://hal.utc.fr/hal-03288795>

Submitted on 16 Jul 2021

HAL is a multi-disciplinary open access archive for the deposit and dissemination of scientific research documents, whether they are published or not. The documents may come from teaching and research institutions in France or abroad, or from public or private research centers.

L'archive ouverte pluridisciplinaire **HAL**, est destinée au dépôt et à la diffusion de documents scientifiques de niveau recherche, publiés ou non, émanant des établissements d'enseignement et de recherche français ou étrangers, des laboratoires publics ou privés.

Multi-omics analysis of hiPSCs-derived HLCs matured on-chip revealed patterns typical of liver regeneration

Mathieu Danoy, Yannick Tauran, Stéphane Poulain, Rachid Jellali, Johanna Bruce, Marjorie Leduc, Morgane Le Gall, Françoise Gilard, Taketomo Kido, Hiroshi Arakawa, et al.

► **To cite this version:**

Mathieu Danoy, Yannick Tauran, Stéphane Poulain, Rachid Jellali, Johanna Bruce, et al.. Multi-omics analysis of hiPSCs-derived HLCs matured on-chip revealed patterns typical of liver regeneration. *Biotechnology and Bioengineering*, Wiley, 2021, 10.1002/bit.27667 . hal-03286480

HAL Id: hal-03286480

<https://hal.uts.fr/hal-03286480>

Submitted on 14 Jul 2021

HAL is a multi-disciplinary open access archive for the deposit and dissemination of scientific research documents, whether they are published or not. The documents may come from teaching and research institutions in France or abroad, or from public or private research centers.

L'archive ouverte pluridisciplinaire **HAL**, est destinée au dépôt et à la diffusion de documents scientifiques de niveau recherche, publiés ou non, émanant des établissements d'enseignement et de recherche français ou étrangers, des laboratoires publics ou privés.

Multi-omics analysis of hiPSCs-derived HLCs matured on-chip revealed patterns typical of liver regeneration

**Mathieu Danoy^{1,2+}, Yannick Tauran^{1,3+}, Stéphane Poulain⁴, Rachid Jellali⁵,
Johanna Bruce⁶, Marjorie Leduc⁶, Morgane Le Gall⁶, Françoise Gilard⁷,
Taketomo Kido⁸, Hiroshi Arakawa⁹, Karin Araya⁹, Daiki Mori¹⁰, Yukio
Kato⁹, Hiroyuki Kusuhara¹⁰, Charles Plessy⁴, Atsushi Miyajima⁸,
Yasuyuki Sakai², Eric Leclerc^{1,5*}**

¹ CNRS UMI 2820; Laboratory for Integrated Micro Mechatronic Systems,
Institute of Industrial Science, University of Tokyo; 4-6-1 Komaba; Meguro-ku;
Tokyo, 153-8505, Japan.

² Department of Chemical System Engineering, graduate school of
Engineering, the University of Tokyo, 7-3-1, Hongo, Bunkyo-ku, Tokyo, 113-
8656, Japan

³ Univ Lyon, Université Claude Bernard Lyon 1, Laboratoire des
Multimatériaux et Interfaces, UMR CNRS 5615, F-69622 Villeurbanne, France

⁴ RIKEN Center for Life Science Technologies, Division of Genomic
Technologies, 1-7-22 Suehiro-cho, Tsurumi-ku, Yokohama, Kanagawa 230-
0045, Japan.

⁵ CNRS UMR 7338, Laboratoire de Biomécanique et Bioingénierie, Sorbonne
universités, Université de Technologies de Compiègne, France

⁶ Plateforme protéomique 3P5, Université de Paris, Institut Cochin, INSERM, CNRS,
F-75014, France

⁷ Plateforme Métabolisme Métabolome, Institute of Plant Sciences Paris-Saclay
(IPS2), CNRS, INRA, Univ. Paris-Sud, Univ. Evry, Univ. Paris-Diderot, Univ. Paris
Saclay, Bâtiment 630 Rue Noetzlin, 91192 Gif-sur-Yvette cedex, France

⁸ Laboratory of Stem Cell Therapy, Institute for Quantitative Biosciences, The
University of Tokyo, 1-1-1 Yayoi, Bunkyo-ku, Tokyo 113-0032, Japan.

⁹ Laboratory of Molecular Pharmacokinetics, Faculty of Pharmacy, Institute of
Medical, Pharmaceutical and Health Sciences, Kanazawa University, Kakuma-machi,
Kanazawa City, Ishikawa, 920-1192, Japan.

¹⁰ Laboratory of Molecular Pharmacokinetics, Graduate School of Pharmaceutical
Sciences, The University of Tokyo, 7-3-1, Hongo, Bunkyo-ku, Tokyo, 113-0033,
Japan.

* Corresponding author: Eric Leclerc

CNRS UMI 2820; Laboratory for Integrated Micro Mechatronic Systems,
Institute of Industrial Science, University of Tokyo; 4-6-1 Komaba; Meguro-ku;
Tokyo, 153-8505, Japan

+ Authors with an equivalent contribution

Abstract

Maturation of human-induced pluripotent stem cells (hiPSCs)-derived hepatocytes-like cells (HLCs) toward a complete hepatocyte phenotype remains a challenge as primitiveness patterns are still commonly observed. In this work, we propose a modified differentiation protocol for those cells which includes a pre-maturation in Petri dishes and a maturation in microfluidic biochip. For the first time, a large range of biomolecular families has been extracted from the same sample to combine transcriptomic, proteomic, and metabolomic analysis. After integration, these datasets revealed specific molecular patterns and highlighted the hepatic regeneration profile in biochips. Overall, biochips exhibited processes of cell proliferation and inflammation (via TGFB1) coupled with anti-fibrotic signaling (via angiotensin 1-7, ATR-2, and MASR). Moreover, cultures in this condition displayed physiological lipid-carbohydrate homeostasis (notably via PPAR, cholesterol metabolism, and bile synthesis) coupled with cell respiration through advanced oxidative phosphorylation (through the over-expression of proteins from the third and fourth complex). The results presented provide an original overview of the complex mechanisms involved in liver regeneration using an advanced in-vitro organ-on-chip technology.

Keywords: iPSCs, hepatocytes, liver, organ-on-chip, differentiation, nanoCAGE, transcriptomics, metabolomics, proteomics

Introduction

Despite significant efforts toward an enhanced maturation hiPSCs-derived (HLCs), primitiveness patterns are still largely observed (Hay *et al.*, 2008; Touboul *et al.*, 2010, Si Tayeb *et al.*, 2010; Kido *et al.*, 2015, Lereau Bernier *et al.*, 2019). Consequently, hiPSCs-derived HLCs are still far from being in a state which would allow them to be used for *in-vitro* studies in the industry. As a complement to conventional culture models, strategies based on tissue engineering using 3D reconstruction and organoids (Takebe *et al.*, 2017) or microscale bioreactors (Giobbe *et al.*, 2015) have been identified as a potential source of improvement for the differentiation of hiPSCs into hepatic cells.

Among those, organ-on-chips, aimed at reproducing the complex human physiology using micro and nanotechnologies (Sosa Hernandez *et al.*, 2018), have allowed proposing a new generation of microfluidic liver models (Kang *et al.*, 2015, Rennert *et al.*, 2015, Jellali *et al.*, 2016). In that regard, the enhancement of the maturation of hiPSCs-derived hepatic cells in a microfluidic biochip has been demonstrated (Danoy *et al.*, 2019). Previous datasets have shown that 7 days of maturation in the biochips were insufficient to obtain a quantifiable and inducible CYP450 activity (Danoy *et al.*, 2019). Nevertheless, the culture in microfluidic biochips exhibited, when compared to Petri dishes, a higher activity of typical liver transcription factors such as ESRRA, HNF1A, HNF4A, TCF4, and CEBPA, as well as a different modulation of pathways related to the extracellular matrix, tissue reorganization, HIF and glycolysis which shows promise for the technology.

In this work, we present an extended maturation of hiPSCs-derived HLCs in microfluidic biochip for 14 days under perfusion and stimulation with OSM. Additionally,

as we observed that the 5cm-long microfluidic biochip that was used in our previous experiment would lead to a largely hypoxic culture condition (Danoy *et al.*, Submitted), we decided to shorten the microfluidic biochip to 1cm. This design has shown its suitability for primary liver human hepatic cultures (Jellali *et al.*, 2016) and allows the reduction of the required number of inoculated cells, which make it more suitable for larger-scale experiments. However, despite a limited amount of biological material in these culture conditions (Around 1.01×10^5 cells per biochip), a large range of different biomolecular family (transcriptome, metabolome, and proteome) have been successfully extracted in a single sample.

The multi-omics approach is essential to understand the key molecular events involved in the stem cell plasticity (Abazova and Krijgsveld, 2017), but until now, the few studies of hepatic differentiation from hiPSCs have mainly focused either on metabolome/transcriptome (Tauran *et al.*, 2019) or more recently on proteomics alone (Hurrel *et al.*, 2019). Here, the multiple datasets have been integrated to identify more accurately the main molecular changes that led eventually to a more mature hepatocyte profile. Finally, a scheme that revealed the biomolecular patterns (promoters, mRNA, proteins, and metabolites) has been proposed. These act as a trigger to specific biological pathways which were found either activated (glycolysis, cell proliferation, inflammation, SMAD, etc.) or inhibited (fibrosis, OXPHO respiration, etc.) under the unique 3D micro-environment offered by the microfluidic biochip culture as compared to the classical 2D Petri dishes.

Results

Cell morphology and tissue characterization

The cultures performed in both Petri dishes (Fig. 1A) and biochips (Fig. 1B) led to the formation of a tissue comprising cells exhibiting a typical hepatocyte morphology with a large nucleus. In biochips, binucleated cells were notably spotted in the middle of the chambers while cells with elongated morphologies were observed close to the walls. The albumin production, both biochips and Petri dishes reached a similar level around 3500 ng/mL/10⁶ cells after 14 days of maturation (Fig. 1C). mRNA levels in Petri dishes and biochips revealed lower levels of ALB in biochips but similar levels of AFP, CYP3A4, and HNF4A in both conditions. When compared to samples issued from Liver Total RNA, both Petri dishes and biochips still exhibited lower levels of maturation notably in terms of CYP3A4 (Fig. 1D).

Immunostainings displayed a higher expression of AFP in Petri dishes when compared to biochips. Most of the cells were found to be positive for CK19 in Petri dishes while only cells on the top of the microstructure were positive in biochips (Fig. 1E). More intense staining for Albumin was observed in biochips when compared to Petri dishes. Expression of BSEP (bile salt export pump, involved in the bile transport and normally located at the canaliculi membranes) and of MRP3, located on the membrane of hepatocytes was also confirmed in the biochip cultures (Fig. 1F).

Functional assays

General capabilities of the tissue in terms of bile acid metabolism were found to be largely enhanced by the culture in microfluidic biochips or by an extended perfusion duration of 14 days (Fig. 2A). Consumption of Cholic Acid (CA) was detected in both Petri dishes and biochips but was found to be significantly more important after 14 days of perfusion in the microfluidic biochips. Resulting productions of Glycocholic Acid (GCA) and Taurocholic Acid (TCA) were only significantly detected in biochips. Interestingly, consumption of Chenodeoxycholic Acid (CDCA) was detected in Petri dishes while a decreasing production from 7 days of perfusion to 14 days was detected in biochips. A production of Glycochenodeoxycholic Acid (GCDCA) was detected on day 14 in both culture modes but was found to be much higher in biochips. Finally, significant consumption of Taurochenodeoxycholic Acid (TCDCA) was observed in biochips after 7 and 14 days of perfusion.

CYP3A4 assay has shown higher activity in biochips when compared to Petri dishes but inducibility with rifampicin was found to be only effective in Petri dishes (Fig. 2B). Metabolisms of phenacetin *via* CYP1A2, of diclofenac *via* CYP2C9 and of coumarin *via* CYP2A6 was confirmed in both Petri dishes and biochips (Fig. 2C). However, the activities of CYP1A2 and CYP2C9 were higher in biochips than in Petri dishes. The extraction of the urea levels from the metabolomic analysis indicated a similar production in both Petri dishes and biochips (Fig. 2D). PAS staining has confirmed the glycogen storage capabilities of the tissue in both Petri dishes and biochips (Fig. 2E).

The profile of cytokines and pro-angiogenic factors produced was evaluated by performing the measurement in biochips, in Petri dishes, and the culture medium (Fig.

2F, detailed results in Supp. Fig. 1). Those results seemed to indicate the consumption of proteins related to the formation of blood vessels and to angiogenesis (ANG, ANGPT2, PECAM-1, and TIE-2) as lower concentrations were found in biochips when compared to what was observed in the culture medium. In parallel, several proteins and cytokines related to angiogenesis (EGF, bFGF, MMP-9, endostatin, and UPAR) and inflammation (ENA-78, GRO, GM-CSF, MCP-3 IL-8, IL-1 beta, and IL-4) were found in higher concentrations in Petri dishes.

Transcriptome analysis

NanoCAGE (Plessy et al., 2010; Poulain et al. 2017) RNA-Seq profiles of cell samples differentiated either in Petri dishes (n=3) or biochips experiments (n=4) have been compared by iDEP8.1 processing (Ge et al., 2018). Differential Gene Expression (DGE) analysis revealed 169 and 236 genes upregulated in Petri dishes and biochips respectively (False Discovery Rate cutoff of 0,1; minimum Fold Change of 2, Supp. File 1). Notably, Transcription Factors (TFs) genes related to CYP1A1, to various transporters such as SLC12A7, SLC4A7, SLC 12A8, SLC 19A2, SLC 25A37 or SLC 2A3, to JUN, MYC, BMP6, ATF3, NFATC1, NFATC2, HCFC1, FOXO3, CTNNB1 (β catenin) or NR4A1 were found to be upregulated in biochips. Several transcripts coding for TFs related to inflammation such as NFKB1A, NFKB1, NFKB2, NFKBIZ, CCL2, CXCL2, TNFRSF10D, TNFAIP3, TGFBI, TGFB2, MAP3K8 were upregulated in biochips. Meanwhile, mRNA levels of TFs such as LYVE1, PECAM1, or ANGPT3 (related to the endothelium), LAMB1, COL16A1 (related to the extracellular matrix and the GP6 signaling) were upregulated in Petri dishes.

By raising the False Discovery Rate cutoff to 0,2 in the DGE analysis, a more restricted list of differentially expressed genes has been obtained for which the heatmap is represented in [Supp. Fig. 2A](#). Pathway Gene Set Enrichment Analysis on this new list using the GO_biological_process geneset allowed to highlight pathways related to liver development, cellular response to oxidative stress, response to lipid, response to chronic inflammation and the regulation of the cell migration involved in angiogenesis sprouting ([Supp. Fig. 2B](#)). Also, the highlighted GO_KEGG pathways were NFKB, TNF, TGF-beta as well as the p53 signaling ([Supp. Fig. 2C](#)). Interestingly, HIF and Hepatitis B signaling were also highlighted by the analysis. Finally, the processes highlighted with the GO_molecular function category were mainly the upregulation of the transcription factor activity as well as processes related to DNA and RNA ([Supp. Fig. 2D](#)).

Motif Activity Response Analysis

NanoCAGE transcriptomic data were processed for Motif Activity Response Analysis (MARA) ([Balwierz, et al., 2014](#)). The top 10 TFs with the highest motif activity extracted from the analysis are listed in [Table 1](#), and the corresponding target genes and signaling pathways are detailed in [Supp-file 1](#). Among those, most were found to have higher activity in biochips (MECP2, TAF1, RELA, SIN3A, MYCN, NFKB1, ZFX, FOSL1, and ZNF711) and only ZEB1 was found to have higher activity in Petri dishes. Based on these TFs, a regulatory network, describing the direct relationship between TFs and their target pathways and genes, could be established ([Fig. 3](#)). Notably, TFs related to inflammation were highlighted (MECP2, RELA, MYCN, NFKB1, ZFX, and FOSL1 *via* the TNFA, TGFB, and NFKB pathways). Besides, TAF1 and ZNF711 were

also featured in the analysis and were linked to the HIF signaling and mitochondrial processing. While they could not be found in the list of the top 10 TFs with the highest activity, PML and PATZ1 were found to be underlying nodes which contributed to bridging the network to important liver functions such as HNF1A and CTNNB1 (Beta Catenin) while associations with the Wnt, HNF3B and NFAT signaling could also be established. Finally, the analysis also revealed a link between MECP2 and several endothelial markers such as ANGPT4 and VEZF1.

Proteomic analysis

The analysis allowed to extract 380 proteins that were differentially expressed in Petri dishes and biochip with p_value below 0,05 among the total of 3186 identified (Fig. 4A, Supp. File 2). Among those, AFP, several collagen proteins, and fibrinogens were found to be over-expressed in Petri dishes while surprisingly, no significant difference could be detected in the expression of CYP450. Amid the top 50 most differentially expressed proteins (Heatmap in Fig. 4B), TIMP1, COL3A1, COL14A1, COL15A1, LG, EMILIN-1 (related to the extracellular remodeling), APOA2 and PLTP (linked to lipid metabolism) were found to be over-expressed in Petri dishes. On the other hand, *MAP3K11*, *IKBIP*, *ASCC3* (related to NFKB activation), *ABLIM3*, *FSCN1*, (actin-related), *AKR1D1* (bile metabolism), *GBA* (glycolipid metabolism), *PLIN2* (perilipin 2, lipid droplet) were found to be over-expressed in biochips. Interestingly, proteins related to the Krebs cycle (*ACO1*, *IDH2*, *SDHA*, *SDHB*, *PCK2*) were also found to be under-expressed in biochips.

By inputting the list of 380 proteins in the Ingenuity Pathway Analysis (Supp. File 3), the modulation of pathways related to the activation of LXR/RXR and FXR/RXR,

to the acute phase response signaling, to the coagulation system and the inhibition of the matrix metalloproteases could be extracted. The top upstream regulators revealed were *TGFβ1*, *iL-6*, and molecules acting on the androgen receptors (dexamethasone, dihydrotestosterone, metribolone). Using the KEGG pathway analysis (Supp. File 2), pathways related to cancer, cell cycle (*CDKN1C*, *MCM2* up-regulated in Petri dishes and *CHEK2*, *ORC3*, *SKP2* up-regulated in biochips), lipid metabolism (PPAR signaling, cholesterol metabolism, and bile synthesis), shear stress, cellular remodeling and reorganization (focal adhesion, ECM-receptor interactions, and tight junctions,) oxidative phosphorylation, iron metabolism (up-regulation of *FTL* and *FTH1* in biochips).

Metabolomics analysis

Based on the OPLS-DA S-plots, 47 metabolites were found to be differentially expressed between Petri dishes and biochips among the 87 identified ones (Fig. 4D-F, with $P < 0.05$ and $VIP > 1$, Supp. File 4). Notably, higher levels of glycerol, cholesterol, malic acid, fumaric acid, succinic acid, aspartic acid (Krebs cycle intermediates), lactic acid and putrescine were found in Petri dishes while higher levels of lipids (lauric acid, oleic acid, caprylic acid, and palmitoleic acid), glucose and amino acids (serine, threonine, lysine, ornithine, phenylalanine, leucine and isoleucine) were observed in biochips.

Those metabolites were mapped with MetaboAnalyst to identify the related metabolic pathways. The analysis revealed that pathways related to the Aminoacyl-tRNA biosynthesis, the alanine aspartate and glutamate metabolism, the fatty acid biosynthesis, the phenylalanine metabolism, and the arginine proline metabolism were

modulated (Supp. File 4). The enrichment analysis highlighted the beta-oxidation, the urea cycle, the spermidine and spermine metabolism, the fatty acid biosynthesis, and the glutathione Metabolism as the top 5 regulated pathways (Supp. File 4).

Discussion

In the present study, the maturation of hiPSCs-derived HLCs was led in a microfluidic environment for 14 days. The protocol has allowed detecting a CYP3A4 activity as well as an improved activity of several cytochromes over Petri dishes and over previously published protocols using biochips (Danoy *et al.*, 2019; Danoy *et al.*, 2020). The multi-omics analysis performed in the biochips revealed a signature, typical of a liver regenerative process, illustrated in Fig. 5.

Analysis of the metabolome in Petri dishes revealed an aerobic respiration profile with important glycolysis as shown by the glucose/lactate ratios and by the over-expression of metabolites and proteins related to the cycle of Krebs in Petri dishes. Notably, proteins from the first and the second protein complex of the respiratory chain were found to be over-expressed in Petri dishes while proteins from the third and the fourth (COX15, ATP6A1) were over-expressed in biochips. The over-expression of proteins from the first complex leads to a high production of ROS (Murphy *et al.*, 2009) which is also consistent with the high levels of pyroglutamate found in Petri dishes and can be linked to the glutathione metabolism (Liu *et al.*, 2014). Also, the over-expression of proteins from the second complex is consistent with the activation of the cycle of Krebs in Petri dishes (Martinez-Reyes *et al.*, 2020) and with a potential response to hypoxia (Pfleger *et al.*, 2015). Finally, the over-expression of proteins from the third

and the fourth complex has been related to a higher OXPHOS capability (Machida, 2018) which might be linked to a profile of higher maturation in biochips.

In both culture modes, the tissue was exposed to high concentrations of insulin and glucose in what is considered a lipogenic stimulation (Schwarz et al., 2003). In biochips, a production of glycerolipids and triglyceric acids, an intense metabolism of steroids, and a synthesis of bile acids from cholesterol were observed. It has often been reported that the metabolism of lipids and the increase of bile acids are strongly related to a process of liver regeneration (Rudnick et al., 2012; Manco et al., 2018; Keitel et al., 2008). After hepatectomy, the liver regeneration process is put in correlation with a transient apparition of a signature attributed to a fatty liver (Schofield et al., 1987; Della Fazia et al., 2018) and is consistent with the overexpression of biomarkers such as PLIN2 (Tsai et al., 2017) and with the high levels bile acids (Puri et al., 2018; Chashmniyam et al., 2019) observed in the biochips.

A major factor of dissociation between the cultures in biochips and Petri dishes was the presence of vascular-related markers and collagen-related proteins in the later (Fig.5). Meanwhile, AGT (angiotensin), a precursor of angiotensin as well as the production of angiotensin were detected in Petri dishes. The resulting consumption of angiotensin or the low levels of angiotensinogen observed in biochips may be related to either a vasoconstriction phenomenon (Consistent with the high levels of mannitol observed, Krishnamurty et al., 1977; Shakat et al., 2012), to the transport of specific solutes (K^+ , Na^+ and Ca^{2+} , as SLC12A7, SLC4A7 and SLC12A8 were found to be upregulated in biochips) or to the regulation of a potential fibrotic state (Pro-fibrotic via *angiotensin 2*, *ATR1* and *TGFB1*; anti-fibrotic via *angiotensin 1-7*, *ATR2* and *MASR*; Shim et al., 2018). It was previously reported that the activation of MAS receptors would contribute to the reduction of the levels of hydroxyproline and collagen A1 in rats

and the increase of vasodilatation (Shim et al., 2018). Those observations would be consistent with the lower levels of trans-4-hydroxy-L-proline and with a potential response to the vasoconstriction phenomenon in biochips. As further confirmations of the observed phenomena, *thrombospondin-1* was found to be upregulated in biochips. This protein is known to be a regulator of blood pressure with a vasopressor activity (Isenberg et al., 2009) and induced by the shear stress which may be resulting from the perfused culture in biochips (Gomes et al., 2005). Besides, angiotensin 2 is known to activate SMAD (Wang et al., 2006) which might be consistent with the modulation of SMAD3 observed in biochips. As signaling attributed to fibrotic and angiogenic pathways were reported to be mostly interconnected in the liver regeneration process (Poisson et al., 2017), the separation between the two phenomena is ambiguous in the biochips. Finally, as angiotensin 2 is a pro-fibrotic factor (Shim et al., 2018), a potential fibrotic state of the tissue in Petri dishes cannot be excluded.

TGF β 1 was identified as an upstream regulator linking potential tissue inflammation, cell proliferation, and a state of liver regeneration. Indeed, the regenerative liver is characterized by sequential stimulations of the TGF β signaling (Apte et al., 2009, Michalopoulos, 2010) but is also involved in inflammation processes with the production of TNF α and IL-6 (Manco et al., 2018) and the activation of NF- κ B (Yang et al., 2015, Leist et al., 1995). The latter is known for its crosstalk with the p53 signaling (Schneider et al., 2010) which may indicate a development towards a tumoral state. This hypothesis might be further enforced as *CDKN1C*, an inhibitor of cell proliferation (Marshall et al., 2005), was found to be over-expressed in Petri dishes. As patterns typical of the progression of the cell cycle were observed in biochips (over-expression of *CDKN2B*, *CD82* mRNA, *CHEK2*, *SKP2*, *CENPF*, and *ORC3*), this led to the identification of a pathway related to cancer in the proteomics and transcriptomics

datasets. However, the typical signature for tumors was not observed in biochips as neither aerobic respiration nor a Warburg effect was identified and as the typical hepatocellular carcinoma protein biomarkers such as *GPC3*, *GP73*, *Annexin 2*, *Osteopontin* (Lou et al., 2017) were not detected. On contrary, lower levels of AFP were found in the transcriptomics and proteomics datasets while GPC3 was also found to under-expressed, which may suggest that the state of liver regeneration is predominant over the potential apparition of a tumoral development.

Conclusion

In the present manuscript, a protocol for the enhancement of the maturation of hiPSCs-derived HLCs has been proposed and combined with an extensive multi-omics analysis approach. These technical advances have allowed characterizing the tissue which has shown an advanced hepatic differentiation, and which was capable to perform the metabolism of several drugs. Production of urea and glycogen were detected while the metabolism of lipids and conjugation of bile acids was also confirmed. In biochips, analysis of the pathways indicated a possible development of the tissue toward a tumoral state but as the typical hepatocellular carcinoma biomarkers were not identified, the option could be excluded. At first sight, the multi-omics analysis led to categorize the tissue in Petri dishes as being in a fibrotic state as shown by the intense production of collagen. However, further investigations revealed a process of liver regeneration in which anti-fibrotic mechanisms were identified. The in-depth analysis performed in this work has allowed a better understanding of the possible crosstalk between liver regeneration processes (including lipogenesis and angiogenesis) and inflammation (along with transient fibrosis and with a steatotic

response) during the maturation of hiPSCs-derived HLCs in a microfluidic environment. Future works including other omics analyses such as epigenetics or Post Translational Modifications but also other approaches like temporal or spatial studies are expected to complete our comprehension of the dynamic processes in hepatocyte differentiation.

Acknowledgments

The project was supported by the iLite ANR-16-RHUS-0005. Stéphane Poulain by the JSPS Grant-in-aid for Scientific Research (S) 16H06328 and Charles Plessy by a grant to RIKEN CLST (DGT) from the MEXT, Japan. We acknowledge the 3P5 proteomic platform (*Université de Paris, Institut Cochin, INSERM, U1016, CNRS, UMR8104, F-75014 PARIS, France*) and François Guillonéau for their precious advice on the proteomic analysis and Cédric Broussard for monitoring the project.

Conflict of interest statement

The authors declare no conflict of interest.

Ethical issue

No ethical approval was required for the work presented in this study.

Online Methods

Complete details on the protocol and corresponding references are given in [Supp. File 5](#).

References

Abazova, N., Krijgsveld, J. (2017) Advances in stem cell proteomics. *Current Opinion in Genetics & Development* 46:149–155.

Apte U, Gkretsi V, Bowen WC, Mars WM, Luo JH, Donthamsetty S, Orr A, Monga SP, Wu C, Michalopoulos GK. Enhanced liver regeneration following changes induced by hepatocyte-specific genetic ablation of integrin-linked kinase. *Hepatology*. 2009 Sep;50(3):844-51.

Balwierz, P. J., Pachkov, M., Arnold, P., Gruber, A. J., Zavolan, M., & van Nimwegen, E. (2014). ISMARA: automated modeling of genomic signals as a democracy of regulatory motifs. *Genome research*, 24(5), 869-884.

Chashmnia, S., Ghafourpour, M., Farimani, A. R., Gholami, A., & Ghoochani, B. F. N. M. (2019). Metabolomic Biomarkers in the Diagnosis of Non-Alcoholic Fatty Liver Disease. *Hepatitis Monthly*, 19(9).

Danoy, M., Bernier, M. L., Kimura, K., Poulain, S., Kato, S., Mori, D., ... & Sakai, Y. (2019). Optimized protocol for the hepatic differentiation of induced pluripotent stem cells in a fluidic microenvironment. *Biotechnology and bioengineering*, 16, 1762-1776

Danoy, M., Poulain, S., Bernier, M. L., Kato, S., Scheidecker, B., Kido, T., Miyajima, A., Sakai, Y., & Leclerc, E. Characterization of liver zonation-like transcriptomic patterns in HLCs derived from hiPSCs in a microfluidic biochip environment, *Biotechnology Progress*, In Revision.

Della Fazia M.A. Servillo G, Foie gras and liver regeneration: a fat dilemma, *Cell Stress*, Vol. 2, No. 7, pp. 162 - 175; doi: 10.15698/cst2018.07.144

Elpek G.O., Angiogenesis and liver fibrosis, *World J Hepatol*. 2015 Mar 27; 7(3): 377–391.

Ge, S.X., Son, E.W. & Yao, R. iDEP: an integrated web application for differential expression and pathway analysis of RNA-Seq data. *BMC Bioinformatics* 19, 534 (2018). <https://doi.org/10.1186/s12859-018-2486-6>

Giobbe G, Michielin F, Luni C, Giulitti S, Martewicz S, Dupont S, Floreani A and

Elvassore N, 2015, Functional differentiation of human pluripotent stem cells on a chip
Nature methods, 12 : 637-643

Gomes N, Legrand C, Fauvel- Lafève F, Shear Stress Induced Release of Von Willebrand Factor and Thrombospondin-1 in Uvec Extracellular Matrix Enhances Breast Tumour Cell Adhesion, Clinical & Experimental Metastasis volume 22, pages 215–223 (2005)

Hay, D. C., Zhao, D., Fletcher, J., Hewitt, Z. A., McLean, D., Urruticoechea-Uriguen, A., ... & Cui, W. (2008). Efficient differentiation of hepatocytes from human embryonic stem cells exhibiting markers recapitulating liver development in vivo. *Stem cells*, 26(4), 894-902.

Hurrell, T., Segeritz, C.P., Vallier, L., Lilley, K.S., Cromarty, A.D. (2019) A proteomic time course through the differentiation of human induced pluripotent stem cells into hepatocyte-like cells. *Scientific Reports*, 9:3270. DOI: 10.1038/s41598-019-39400-1.

Isenberg J, Qin Y, Maxhimer J, Sipes J, Despres D, Schnermann J, Frazier W, and Roberts D, Thrombospondin-1 and CD47 Regulate Blood Pressure and Cardiac Responses to Vasoactive Stress, *Matrix Biol.* 2009 March ; 28(2): 110–119. doi:10.1016/j.matbio.2009.01.002.

Jellali, R., Bricks, T., Jacques, S., Fleury, M.J., Paullier, P., Merlier, F., et al. Long-term human primary hepatocyte cultures in a microfluidic liver biochip show maintenance of mRNA levels and higher drug metabolism compared with petri cultures. *Biopharm Drug Dispos* 37, 264, 2016.

Kang, Y. B., Sodunke, T. R., Lamontagne, J., Cirillo, J., Rajiv, C., Bouchard, M. J., & Noh, M. (2015). Liver sinusoid on a chip: Long-term layered co-culture of primary rat hepatocytes and endothelial cells in microfluidic platforms. *Biotechnology and bioengineering*, 112(12), 2571-2582.

Keitel V., Kubitz R., Häussinger D. Endocrine and paracrine role of bile acids. *World J. Gastroenterol.* 2008;14:5620–5629

Kido, T., Kouji, Y., Suzuki, K., Kobayashi, A., Miura, Y., Chern, E. Y., ... & Miyajima, A. (2015). CPM is a useful cell surface marker to isolate expandable bi-potential liver progenitor cells derived from human iPS cells. *Stem cell reports*

Krishnamurty, V. S., Adams, H. R., Smitherman, T. C., Templeton, G. H., & Willerson, J. T. (1977). Influence of mannitol on contractile responses of isolated perfused arteries. *American Journal of Physiology-Heart and Circulatory Physiology*, 232(1), H59-H66.

Leist M, Gantner F, Jilg S, Wendel A. Activation of the 55 kDa TNF receptor is necessary and sufficient for TNF-induced liver failure, hepatocyte apoptosis, and nitrite release., *J Immunol.* 1995 Feb 1;154(3):1307-16.

Lereau- Bernier, M., Poulain, S., Tauran, Y., Danoy, M., Shinohara, M., Kimura, K., ... & Sakai, Y. (2019). Profiling of derived-hepatocyte progenitors from induced pluripotent stem cells using nanoCAGE promoter analysis. *Biochemical engineering journal*, 142, 7-17.

Liu, Y., Hyde, A. S., Simpson, M. A., & Barycki, J. J. (2014). Emerging regulatory paradigms in glutathione metabolism. In *Advances in cancer research* (Vol. 122, pp. 69-101). Academic Press.

Lou, J., Zhang, L., Lv, S., Zhang, C., & Jiang, S. (2017). Biomarkers for hepatocellular carcinoma. *Biomarkers in cancer*, 9, 1179299X16684640.

Machida, K. (2018). Pluripotency transcription factors and metabolic reprogramming of mitochondria in tumor-initiating stem-like cells. *Antioxidants & redox signaling*, 28(11), 1080-1089.

Manco R, Leclercq I, Clerbaux L-A, Liver Regeneration: Different Sub-Populations of Parenchymal Cells at Play Choreographed by an Injury-Specific Microenvironment, *Int J Mol Sci.* 2018 Dec; 19(12): 4115.

Marshall A, Rushbrook S, Morris L, Scott I, Vowler S, Davie S, Coleman N, and Alexander G, Hepatocyte Expression of Minichromosome Maintenance Protein-2 Predicts Fibrosis Progression After Transplantation for Chronic Hepatitis C Virus: A Pilot Study , *Liver Transplantation*, Vol 11, No 4 (April), 2005: pp 427-433

Martínez-Reyes, I., & Chandel, N. S. (2020). Mitochondrial TCA cycle metabolites control physiology and disease. *Nature Communications*, 11(1), 1-11.

Michalopoulos G.K., Liver Regeneration after Partial Hepatectomy, Critical Analysis of Mechanistic Dilemmas, *Am J Pathol.* 2010 Jan; 176(1): 2–13.

Murphy M, How mitochondria produce reactive oxygen species, *Biochem J.* 2009 Jan 1; 417(Pt 1): 1–13.

Pfleger, J., He, M., & Abdellatif, M. (2015). Mitochondrial complex II is a source of the reserve respiratory capacity that is regulated by metabolic sensors and promotes cell survival. *Cell death & disease*, 6(7), e1835-e1835.

Plessy C, Bertin N, Takahashi H, Simone R, Salimullah M, Lassmann T, et al., Linking promoters to functional transcripts in small samples with nanoCAGE and CAGEscan, *Nat. Methods*, 2010, 7(7), 528.

Poisson J, Lemoine S, Boulanger C, Durand F, Moreau R, Valla D, Rautou P-E, Liver sinusoidal endothelial cells: Physiology and role in liver diseases, *Journal of Hepatology* 2017 vol. 66 j 212–227

Poulain S, Kato S, Arnaud O, Morlighem JE, Suzuki M, Plessy C, et al., NanoCAGE: a method for the analysis of coding and noncoding 50-capped transcriptomes. In: Napoli S. (eds) *Promoter Associated RNA. Methods in Molecular Biology*, vol 1543. Humana Press, New York, NY, 2017, pp. 57–109.

Puri P, Daita K, Joyce A, Mirshahi F, Santhekadur P, Cazanave S, Luketic V, Mohammad S, Siddiqui M, Boyett S, Min H-K, Kumar D, Kohli R, Zhou H, Hylemon P, Contos M, Idowu M, Sanyal A, The presence and severity of nonalcoholic steatohepatitis is associated with specific changes in circulating bile acids, *Hepatology*, 67:2, 2018

Rennert, K., Steinborn, S., Gröger, M., Ungerböck, B., Jank, A. M., Ehgartner, J., ... & Peters, F. T. (2015). A microfluidically perfused three dimensional human liver model. *Biomaterials*, 71, 119-131.

Rudnick D, Davidson N, Functional Relationships between Lipid Metabolism and Liver Regeneration, *Int J Hepatol*. 2012; 2012: 549241.

Shawkat, H., Westwood, M. M., & Mortimer, A. (2012). Mannitol: a review of its clinical uses. *Continuing education in anaesthesia, critical care & pain*, 12(2), 82-85.

Schneider, G., Henrich, A., Greiner, G., Wolf, V., Lovas, A., Wieczorek, M., ... & Weih, F. (2010). Cross talk between stimulated NF- κ B and the tumor suppressor p53. *Oncogene*, 29(19), 2795-2806.

Schofield, P. S., Sugden, M. C., Corstorphine, C. G., & Zammit, V. A. (1987). Altered interactions between lipogenesis and fatty acid oxidation in regenerating rat liver. *Biochemical Journal*, 241(2), 469-474.

Schwarz J. M., Linfoot P., Dare D. & Aghajanian K. (2003). Hepatic de novo lipogenesis in normoinsulinemic and hyperinsulinemic subjects consuming high-fat, low-carbohydrate and low-fat, high-carbohydrate isoenergetic diets. *American Journal of Clinical Nutrition* 77, 43–50.

Si-Tayeb, K., Noto, F. K., Nagaoka, M., Li, J., Battle, M. A., Duris, C., ... & Duncan, S. A. (2010). Highly efficient generation of human hepatocyte-like cells from induced pluripotent stem cells. *Hepatology*, 51(1), 297-305.

Shim K, Eom Y, Kim M, Kang S, & Baik S, Role of the renin-angiotensin system in hepatic fibrosis and portal hypertension , Korean J Intern Med 2018;33:453-461,

Sosa-Hernández JE, Villalba-Rodríguez AM, Romero-Castillo KD, Aguilar-Aguila-Isaías MA, García-Reyes IE, Hernández-Antonio A, Ahmed I, Sharma A, Parra-Saldívar R, Iqbal HMN. Organs-on-a-Chip Module: A Review from the Development and Applications Perspective. *Micromachines (Basel)*. 2018 Oct 22;9(10):536.

Takebe, T., Sekine, K., Kimura, M., Yoshizawa, E., Ayano, S., Koido, M., et al. Massive and reproducible production of liver buds entirely from human pluripotent stem cells. *Cell Rep* 21, 2661, 2017.

Tauran, Y., Poulain, S., Lereau-Bernier, M., Danoy, M., Shinohara, M., Segard, B.D., Kato, S., Kido, T., Miyajima, A., Sakai, Y., Plessy, C., Leclerc, E. (2019) Analysis of the transcription factors and their regulatory roles during a step-by-step differentiation of induced pluripotent stem cells into hepatocyte-like cells. *Mol. Omics*, 15, 383. DOI: 10.1039/c9mo00122k.

Touboul, T., Hannan, N. R., Corbineau, S., Martinez, A., Martinet, C., Branchereau, S., ... & Weber, A. (2010). Generation of functional hepatocytes from human embryonic stem cells under chemically defined conditions that recapitulate liver development. *Hepatology*, 51(5), 1754-1765.

Tsai T, Chen E, Li L, Saha P, Lee H, Huang L, Shelness G, Chan L, and Hung-Junn Chang B, The constitutive lipid droplet protein PLIN2 regulates autophagy in liver, *Autophagy*. 2017; 13(7): 1130–1144.

Yang Y.M., Ph.D. and Seki E., TNF α in liver fibrosis, *Curr Pathobiol Rep*. 2015 Dec; 3(4): 253–261.

Wang W, Huang X, Canlas E, Oka K, Truong L, Deng C, Bhowmick N, Ju W, Bottinger E, and Lan H, Essential Role of Smad3 in Angiotensin II–Induced Vascular Fibrosis, *Circ Res*. 2006 Apr 28; 98(8): 1032–1039.

Table 1: Top 10 TF motifs extracted in the comparison between biochips and Petri dishes by ISMARA, sorted by z-value.

“TF motif” represents a set of transcription factors with similar target nucleotide sequence patterns identified by CAGE. “PCC” is the gene with strongest Pearson correlation coefficient for the identified TF motif. “Pattern” describes the nucleotide sequence pattern of the motif for the PCC.

TF motif	Z-value of motif activity	PCC	Up	Pattern	Function
MECP2	2,08	MECP2	Biochip	CCCGGAG	NFKB, NFAT, FOXO and JNK pathways
TAF1	1,93	TAF1	Biochip	GCCGCCA TCTT	HIF, Beta-catenin, Mitochondrial processes, glucokinase regulation
ZEB1	1,72	ZEB1	Petri	CTCACCTG	EMT
RELA	1,49	RELA	Biochip	GGGAATTT CCC	NFKB, MAPK, JNK and STAT3 pathways, inflammation
SIN3A_CHD1	1,41	SIN3A	Biochip	GGAGGCG GAGGTGG GAGAG	E cadherin stabilisation, Wnt, SMAD2 and NFAT pathways, cell defense
MXI1_MYC_MYCN	1,24	MXI1	Biochip	CCACGTG	SMAD2 and MYC pathways, glucose, fatty acid reactomes
NFKB1	1,19	NFKB1	Biochip	GGGGAAT CCCC	NFKB response
ZFX	1,18	ZFX	Biochip	GGGGCCG AGGCCTG	HDAC, VEGF, Wnt and IL2 pathways, NFKB complex
FOSL1	1,17	FOSL1	Biochip	GTGAGTC A	Response to inflammation (TNF, MAPK), response to nitrogen level
ZNF711_TFAP2A_TFAP2D	1,17	ZNF711	Biochip	AGGCCTA G	HIF and SMAD2 pathway Interactions between Notch and Wnt

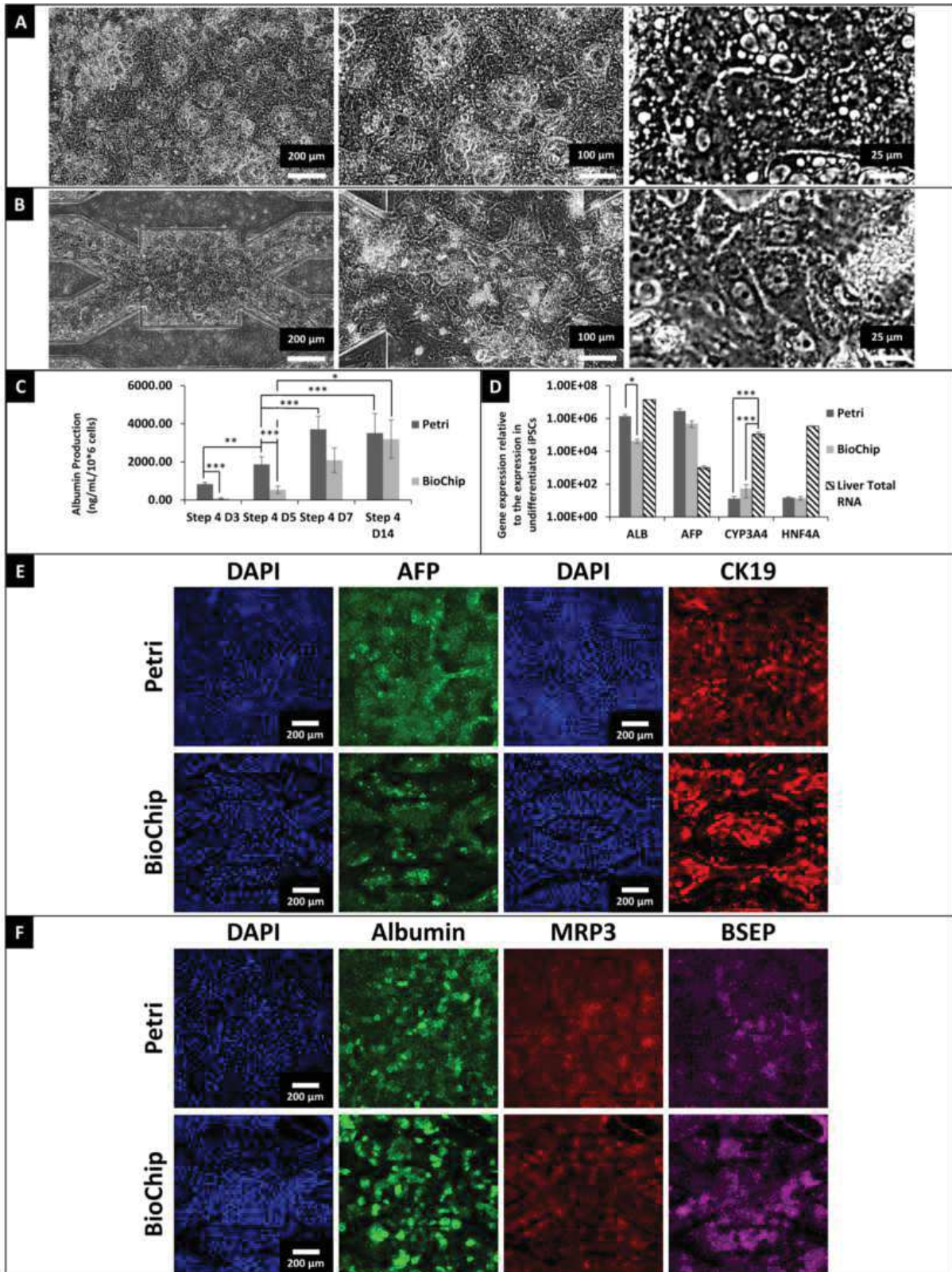


Fig. 1

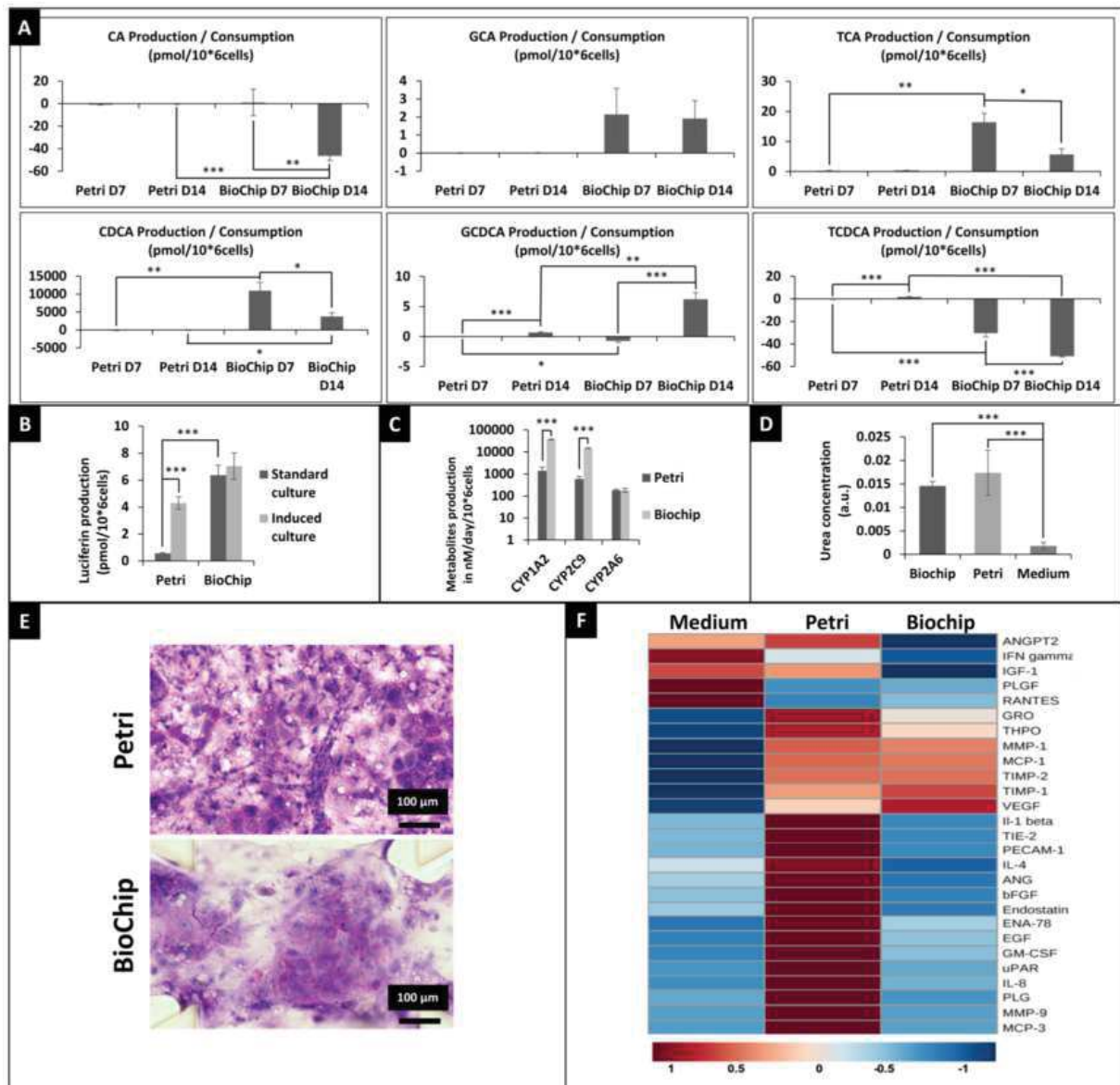


Fig.2

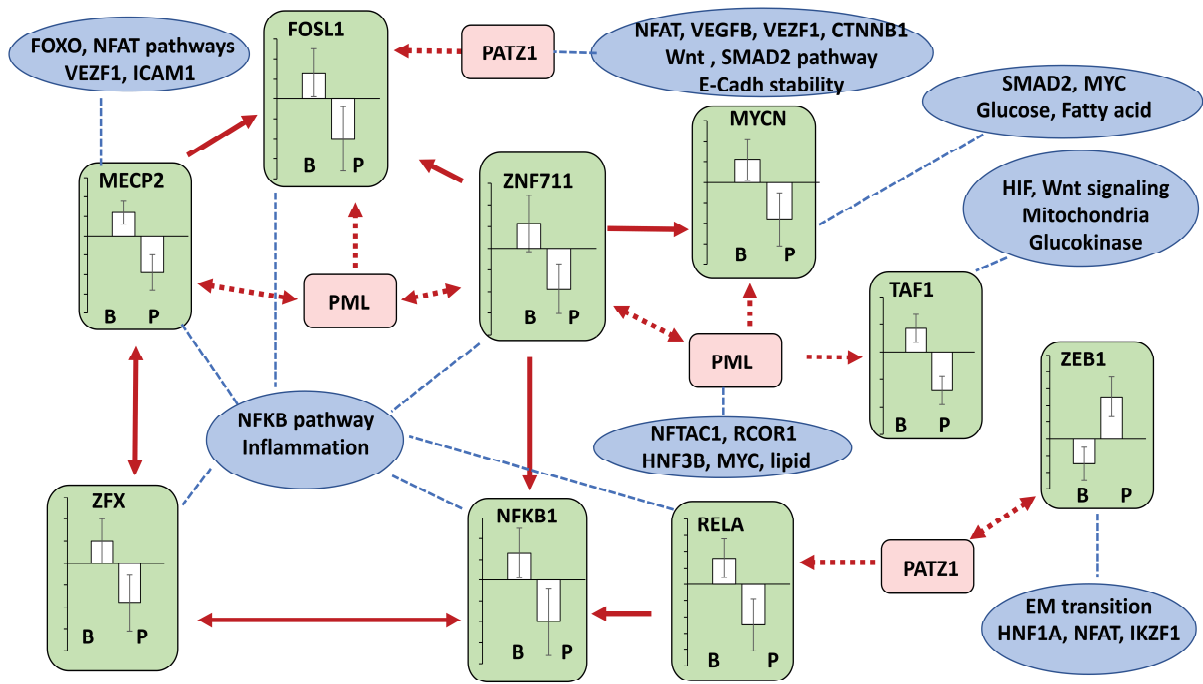


Fig.3

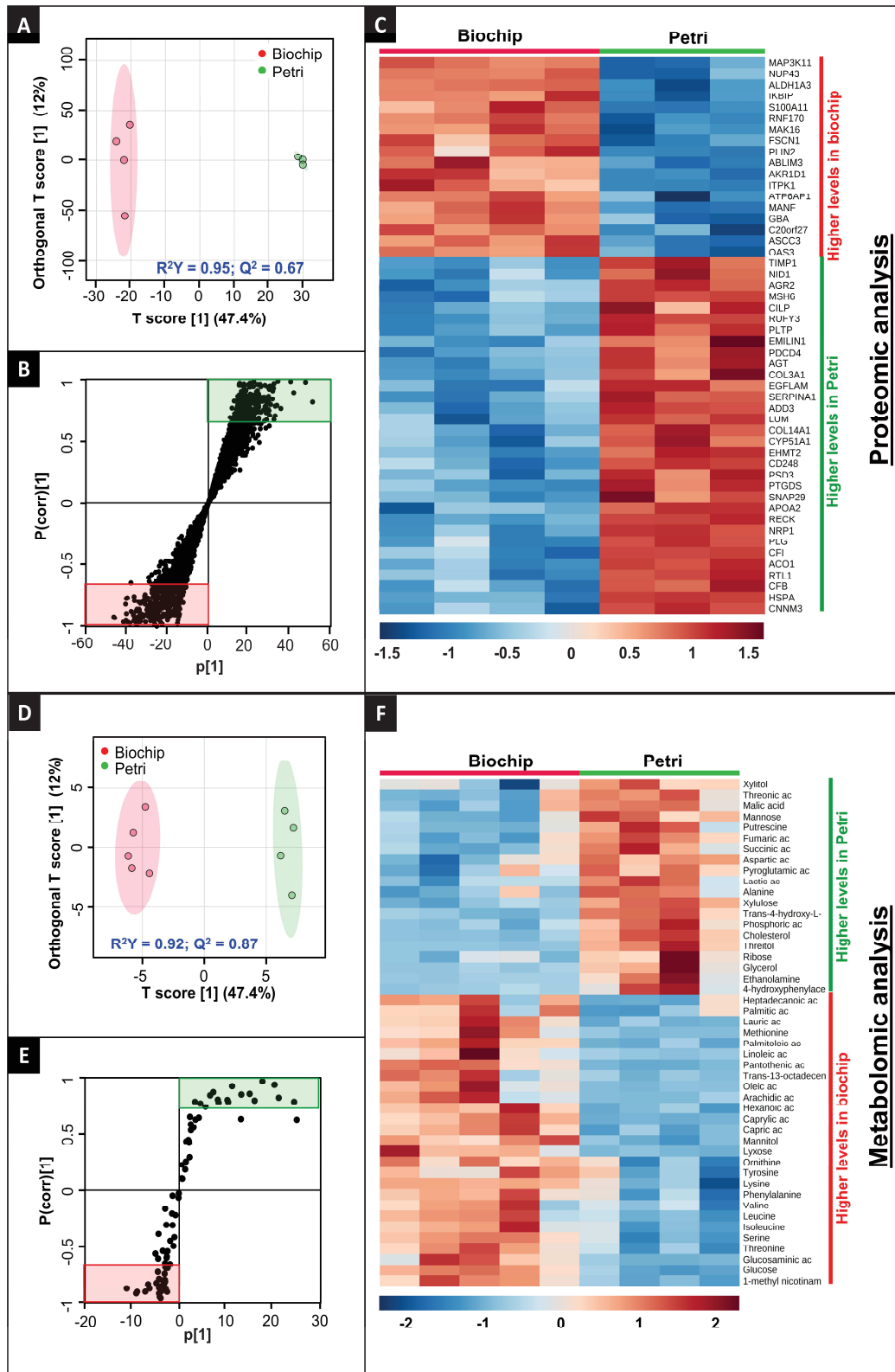


Fig.4

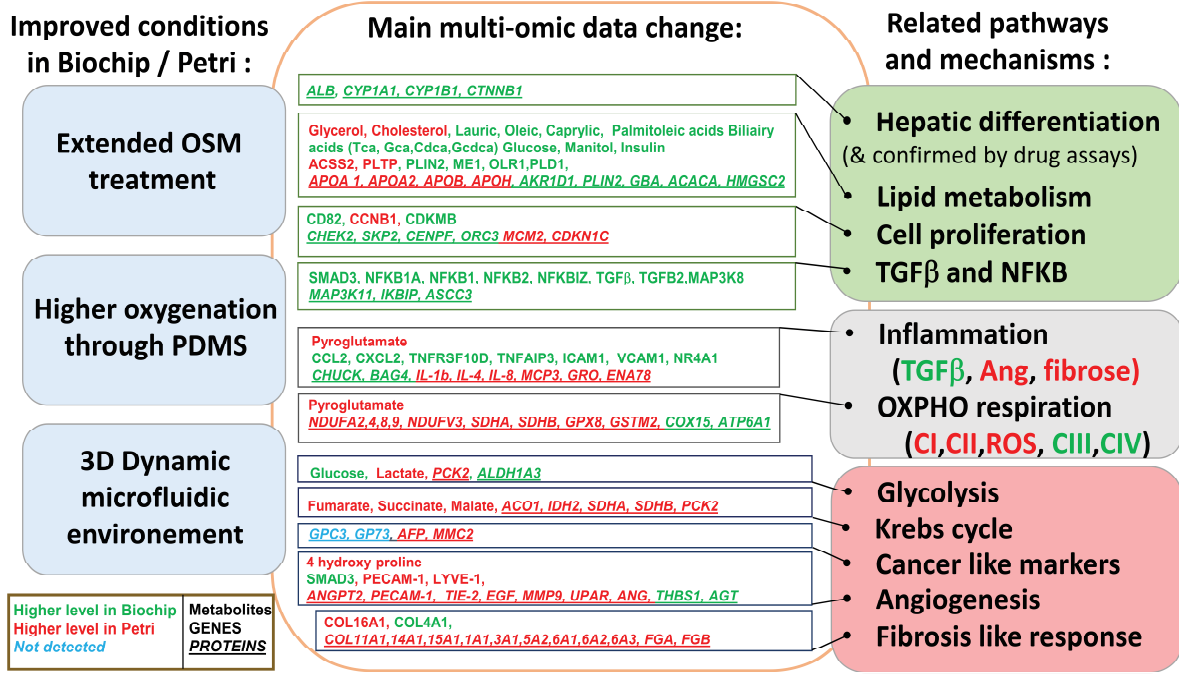


Fig.5